Carbohydrate Polymers 97 (2013) 65–73

Contents lists available at SciVerse ScienceDirect

Carbohydrate Polymers

journal homepage: www.elsevier.com/locate/carbpol

Fabrication of sonicated chitosan nanofiber mat with enlarged porosity for use as hemostatic materials☆

Bon Kang Gu[a,1], Sang Jun Park[a,1], Min Sup Kim[a], Chang Mo Kang[a], Jong-Il Kim[b], Chun-Ho Kim[a,*]

[a] Laboratory of Tissue Engineering, Korea Institute of Radiological and Medical Science, 215-4, Gongneung, Nowon, Seoul 139-240, Republic of Korea
[b] Department of Food and Microbial Technology, Seoul Women's University, Seoul 139-774, Republic of Korea

ARTICLE INFO

Article history:
Received 8 January 2013
Received in revised form 16 April 2013
Accepted 17 April 2013
Available online 30 April 2013

Keywords:
Chitosan nanofibers
Porosity control
Electrospinning
Ultra-sonication
Tissue engineering
Hemostatics

ABSTRACT

Electrospinning of pure chitosan was employed to obtain a nanofibrous hemostatic material. Owing to the water-solubility of the resulting acidic chitosan nanofibers, the optimum neutralization conditions were identified by testing various alkaline solutions, so that an insoluble material could be achieved. The pore size and thickness of the neutralized chitosan nanofibers mat could be controlled using ultra-sonication. The porosity of the chitosan mat was increased from 79.9% to 97.2% with ultra-sonication treatment for 1 min, and the water absorption time decreased from 110 s to 9 s. The blood clotting efficiency measured for the sonicated chitosan nanofiber mat was 1.35- and 3.41-fold better than the efficiencies of the Surgicel® and chitosan sponge, respectively. In addition, the proliferation of normal human dermal fibroblasts on the sonicated nanofiber mat was found to be 1.4-fold higher than that on the non-sonicated material after 7 days of culture.

1. Introduction

Many biodegradable and biocompatible natural polymers have been used to prepare scaffolds for use in tissue engineering and drug delivery applications (Hubbel, 1995; Kim et al., 2011; Park, Lee, & Kwon, 2010; Xie, MacEwan, Li, Sakiyama-Elbert, & Xia, 2009). Among these natural polymers, chitosan has attracted considerable interest owing to its advantageous biological properties (Bhattarai et al., 2009; Desai, Kit, Li, & Zivanovic, 2008; Sangsanoh et al., 2010).

Chitosan is prepared by N-deacetylation of chitin, which is the second most abundant polysaccharide found in nature (Muzzarelli, Greco, Busilacchi, Sollazzo, & Gigante, 2012; Muzzarelli, 2009). Chitosan has been demonstrated to be an invaluable material in the fields of biomedical engineering and biotechnology because of its wound healing effect, in addition to good biocompatibility and biodegradability, and is currently used in a wide variety of applications such as cosmetics and medical materials (Jayakumar, Prabaharan, Nair, & Tamura, 2010; Jayakumar, Chennazhi, Muzzarelli, Tamura, Nair, & Selvamurugan, 2010; Muzzarelli, 2011). The safety and biodegradability of chitosan have been recently reviewed (Baldrick, 2010; Dash, Chiellini, Ottenbrite, & Chiellini, 2011; Kean & Thanou, 2010). A number of studies have demonstrated chitosan to be a potential material for use in hemostatic applications (Chen, Wang, Wei, Mo, & Cui, 2010; Cooper, Jana, Bhattarai, & Zhang, 2010; Ueno, Mori, & Fujinaga, 2001). The mechanism by which it promotes hemostasis is known to involve the agglutination of blood proteins and platelet activation for encouraging fibrin clot formation (Fischer et al., 2005; Janvikul, Uppanan, Thavornyutikarn, Krewraing, & Prateepasen, 2006; Lord, Cheng, McCarthy, Jung, & Whitelock, 2011), possibly due to the intrinsic polycationic properties of chitosan and its nonspecific binding to cell membranes (Yang et al., 2008). Research aimed at elucidating the details of the process is still ongoing (Gu et al., 2010; Malette, Quigley, Gaines, Johnson, & Rainer, 1983; Ong, Wu, Moochhala, Tan, & Lu, 2008). Commercially available chitosan-based hemostatic dressings (Clo-Sur PAD, Scion Cardio-Vascular, USA & Instant Clot Pad, Cosmo Medical Inc., Taiwan) have several shortcomings that limit their clinical application, including the presence of a trace acidulous odor due to the use of acetic acid as a processing solvent. They also have an inability to retain their shape under compression owing to their fragility (Kang et al., 2011), meaning that the acidic chitosan hemostatic agents are prone to collapse at the wound site. Therefore, a safer and more effective means by which to exploit

* Corresponding author at: Laboratory of Tissue Engineering, Korea Institute of Radiological and Medical Sciences, 215-4, Gongneung-Dong, Nowon-Gu, Seoul 139-706, Republic of Korea. Tel.: +82 2 970 1319; fax: +82 2 970 1317.
E-mail address: chkim@kcch.re.kr (C.-H. Kim).

[1] Equally contributed.

0144-8617/$ – see front matter © 2013 The Authors. Published by Elsevier Ltd. All rights reserved.
http://dx.doi.org/10.1016/j.carbpol.2013.04.060

the hemostatic properties of chitosan in a clinical setting is highly sought after.

Electrospinning is a versatile technique that can be used to produce nanoscale fibers from a wide variety of natural and synthetic polymers (Doshi & Renekar, 1995; Dzenis, 2004; Greiner & Wendorff, 2007; Lee, Lee, Jin, & Park, 2010; Reneker & Chen, 1996). Nanofibers have a number of desirable characteristics such as a high area to volume ratio. Many researchers have reported the use of chitosan-based nanofiber mats for a variety of biomedical applications, including tissue templates, artificial organs, and wound dressings (Elsabee, Naguib, & Morsi, 2012; Geng, Kwon, & Jang, 2005; Klossner, Queen, Coughlin, & Krause, 2008; Ohkawa, Cha, Kim, Nishida, & Yamamoto, 2004; Schiffman & Schauer, 2008). Chitosan is able to be electrospun into fibers with diameters in the range of 100 nm to a few microns; however, the pores within materials consisting nanofibers are extremely small due to the random deposition of the fibers. This results in such mats generally exhibiting super-hydrophobicity (Tang, Wang, & He, 2009). In addition, the density of the nanofibers restricts cell growth and mass transport of nutrients and metabolic waste, and also causes slow absorbance of water or blood through the nanofibers structure. To obtain a polymer nanofiber mat that overcomes these problems, Lee et al. reported an ultra-sonication treatment that was able to increase pore size and the thickness of the synthetic polymeric nanofibers (Lee et al., 2011).

In this study, we investigated the potential of chitosan nanofibers mats with enhanced porosity for use as hemostatic wound dressings. Acid-free chitosan nanofiber mats were fabricated using neutralization with subsequent electrospinning, and, in order to improve the absorptivity of the material to water, an ultra-sonication method was then employed. The effects of the ultra-sonication treatment on porosity, wettability, and blood clotting efficiency of the chitosan nanofiber mats were investigated, and the viability of normal human dermal fibroblasts (NHDFs) cultured on the materials was evaluated.

2. Experimental

2.1. Materials

Chitosan powder (average Mw, 370 kDa; deacetylation degree 85%), trifluoroacetic acid (TFA, ~99% purity), dichloromethane (DCM), Na_2CO_3, and NaOH were purchased from Sigma–Aldrich (St. Louis, MO, USA). Chitosan powder was purified to remove impurities; that is, 1% chitosan powder (wt/v) was dissolved in 1% acetic acid (v/v) at 4 °C until the solution became transparent, and homogeneous. The resulting chitosan solution was filtered through glass filters (25G2) to remove impurities. The filtrate was precipitated by adding 1 M NaOH, and washed by deionized water until neutral pH. Then the resulting chitosan was lyophilized for 2 days (Kim, Park, Gu, & Kim, 2012).

Normal human dermal fibroblast cells (NHDFs, MCTT, Korea) were used to evaluate cell proliferation and morphology. The fibroblasts were cultured in fibroblast growth medium (FGM) containing 2% fetal bovine serum (FBS), 0.1% insulin, recombinant human fibroblast growth factor-B (rhFGF-B), and 0.1% GA-1000 antibiotic solution (Lonza, USA). Cells were used from passages 9. Adherent NHDFs were rinsed thoroughly with Dulbecco's phosphate buffered saline (DPBS, WelGENE, Korea) and detached using 0.05% trypsin-EDTA (Gibco, USA) prior to seeding onto the materials.

2.2. Fabrication of chitosan nanofibers by electrospinning

The chitosan nanofiber mats were prepared directly on an aluminum foil-covered drum collector of the electrospinning system. Briefly, a 5% (w/v) chitosan solution was prepared by dissolving it in TFA/DCM (7:3, v/v). The solution was transferred to a 10 mL syringe fitted with a metal needle (21-gauge). The needle was located at a distance of 15 cm from the collector. A syringe pump (KD Scientific, USA) was used to feed the chitosan solution to the needle tip at a feed rate of 1.0 ml/h. During electrospinning, the needle of the syringe was subjected to a voltage of 21 kV relative to the ground collector using a high-voltage power supply (Wookyung Tech, Korea). Electrospinning was conducted in a humidity of less than 30% and a temperature of 20–24 °C. Residual solvent from the chitosan nanofiber mats were removed by drying in a vacuum oven at 30 °C for at least 1 day.

2.3. Neutralization of chitosan nanofiber mats

As the chitosan nanofiber mats were soluble in water, they were neutralized after formation in order to prevent their dissolution in aqueous medium. Various different alkali solutions were used, namely, Na_2CO_3, NH_3, and NaOH. The neutralization was performed by immersing each mat in 5 M Na_2CO_3, 29% NH_3 in aqueous solution, or 3 M NaOH in an aqueous solution of methanol for 3 h, 30 min, and 10 min, respectively. After immersion in these solutions, the nanofiber mats were repeatedly washed with distilled water until a pH 7 was obtained for the washings. They were then freeze-dried for 1 day.

2.4. Porosity control of chitosan nanofiber mats using ultra-sonication

The neutralized chitosan nanofiber mat (2 cm × 2 cm or circular diameter 15 mm) was immersed in 10 mL distilled water at 4 °C (ice bath) after prewetted by distilled water for 10 min. Ultra-sonication of wetted chitosan nanofiber was then carried out using a VCX 750 ultra-sonicator (Sonics & Materials Inc., USA). The ultra-sonication time was controlled in the range of 1–4 min with a power of 225 W. For further characterization, the chitosan nanofiber mats subjected to 1 min ultra-sonication treatment was chosen for analysis.

2.5. Preparation of chitosan sponge

The chitosan sponge was fabricated as described in our previous studies (Kim et al., 2012). Briefly, the chitosan solutions, prepared by dissolving 2% purified chitosan (wt/v) in 1% acetic acid (v/v), were ultra-sonicated at 4 °C for 30 min using an ultra-sonicator to achieve different molecular-weight solutions. Then, ultra-sonicated 2% (wt/v) chitosan solutions were diluted to 1% chitosan by adding 16% (v/v) butanol (dissolved in 1% acetic acid) and stirring for 1 h. The resulting chitosan solutions were lyophilized for 1 day, and then washed sequentially with 100%, 70% and 50% ethanol, and deionized water for 1 h each. The chitosan scaffolds were then freeze-dried for 1 day.

2.6. Water absorption and blood clotting studies

The water absorption time and initial contact angle of sonicated and non-sonicated chitosan nanofiber mats were measured using a digital contact angle instrument with a CCD camera (Phoenix 150, SEO, Korea).

The blood clotting studies were performed according to previously reported methods, with some modifications (Madhumathi et al., 2010; Shih et al., 2006). Blood was obtained from New Zealand white rabbits. The blood clotting efficiency (hemoglobin binding) of the chitosan nanofiber mats was compared with a Surgicel® (Johnson & Johnson Medical, USA), chitosan sponge and commercial gauze. The samples were cut into 1 cm × 1 cm squares and placed into 50 ml tubes. Whole blood was mixed with the anticoagulant

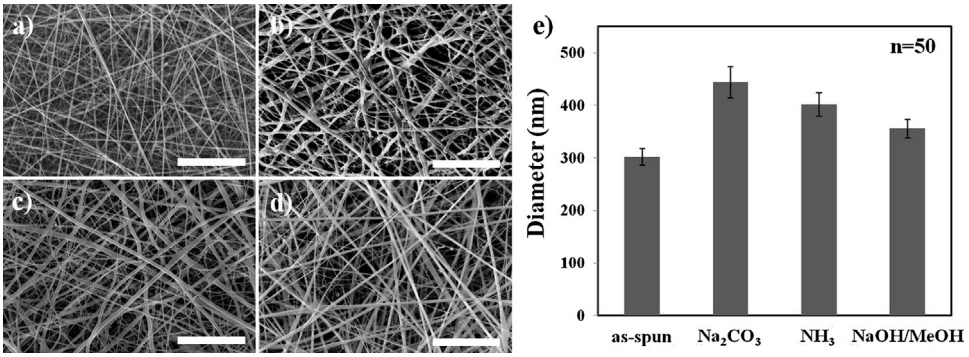

Fig. 1. FE-SEM micrographs of the chitosan nanofibers: (a) non-neutralized as-spun chitosan nanofibers mat, and after neutralization with (b) 5 M Na_2CO_3, (c) 29% NH_3 and (d) 3 M NaOH in MeOH alkali aqueous solutions, (e) distribution of nanofiber diameters (scale bar: 10 μm).

agent acid citrate dextrose (ACD) at a ratio of 9:1. A 200 μl sample of this blood was slowly dropped to each sample, followed by the addition of 20 μl of 0.2 M $CaCl_2$ solution to initiate blood clotting. The samples were maintained at 37 °C for 10 min then 25 ml of deionized water was carefully added to each tube without disturbing the clot. Subsequently, 15 ml of solution from the tube was taken and placed in a fresh 50 ml centrifuge tube. The solution was centrifuged at 1000 rpm for 1 min and then the supernatant was collected and incubated at 37 °C for 1 h.

200 μl aliquots of the solution were added to the wells of a 96-well plate and the level of hemoglobin binding was determined by measuring the absorption at 540 nm using a plate reader (Spectra Max M2e, Molecular Devices, USA), which corresponded to the amount of hemolyzed red blood cells that were not incorporated into the clot.

2.7. Other characterizations

The surface and cross sectional morphology of the chitosan nanofiber mats (sonicated and non-sonicated) were analyzed using field emission scanning electron microscopy (FE-SEM, Mira II, Tescan, Czech Republic) after sputter coating with gold for 5 min. All samples were examined at an acceleration voltage of 15 kV. The images were analyzed using the Image pro plus software (USA) to assess the mat morphology and thickness, and the diameter of the chitosan nanofibers.

The mechanical properties of the chitosan nanofiber mats were measured using a mechanical testing machine (AGS-J 500N, Shimadzu, Japan) at a crosshead speed of 10 mm/min. The samples were cut into a strip-shape (1 cm × 4 cm) and stress versus strain curves were obtained ($n = 10$).

Measurements of porosity and pore size distribution of the sonicated and non-sonicated mats were obtained using mercury porosimetry (AutoPore IV 9500, Micromeritics, USA).

2.8. In vitro cell studies

Circular samples 15 mm in diameter were cut from the sonicated chitosan mat and fixed in the wells of a 24-well cell culture plate with stainless steel rings.

They were sterilized with 70% ethanol and UV irradiation, and then washed three times with PBS. NHDFs were seeded onto the samples at a density of 1×10^4 cells/well, and the culture medium was changed every 3 days. Cell viability was evaluated at 1, 4 and 7 days using cell counting kit-8 (CCK-8, Dojindo, Japan). At the appointed time, the culture medium was removed. The cells were washed three times with Dulbecco's phosphate-buffered saline (DPBS) to remove the residual culture media. Each sample was then incubated with 300 μl culture medium and 30 μl of CCK-8 solution at 37 °C for 4 h. The optical density (OD) of each sample was measured at 450 nm using a plate reader (Molecular Devices, Sunnyvale, USA). At each time point, the cells on the chitosan mat were fixed with 2.5% glutaraldehyde and 2% formaldehyde in PBS overnight at 4 °C. The fixed cells were then dehydrated by immersing in increasing concentration of ethanol in water (30–100%) for 30 min each. The cell morphology on the different samples was observed using FE-SEM.

2.9. Statistical analysis

Quantitative data were obtained in triplicate and are presented as mean ± standard deviation. Significant differences ($p < 0.05$) between experimental groups were determined by a Student's *t*-test.

3. Results and discussion

Chitosan nanofiber mats were electrospun from a solution consisting of concentrated TFA and DCM (7:3, v/v). The productivity efficiency of an as-spun chitosan nanofiber mats were found to be 1.2 ± 0.3 μg/cm^2 with ~80 μm thickness ($n = 4$). FE-SEM images of the surface morphology of the as-spun chitosan nanofibers (Fig. 1(a)) show a smooth and bead-free structure, with the average nanofiber diameter measured to be 301.9 ± 30.4 nm. Owing to the acidity of the produced material, even a single drop of water on the chitosan surface immediately destroyed the nanofibers structure.

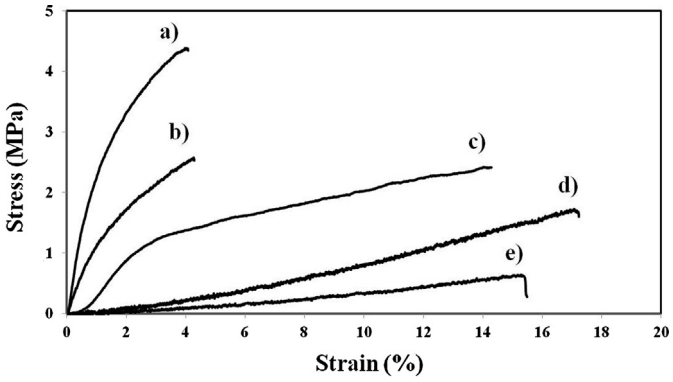

Fig. 2. Mechanical properties of chitosan nanofibers mat and, neutralized and sonicated chitosan nanofibers mat in dry and wet state: (a) neutralized dry state, (b) sonicated dry state, (c) as-spun nanofibers, (d) neutralized wet state, and (e) sonicated wet state.

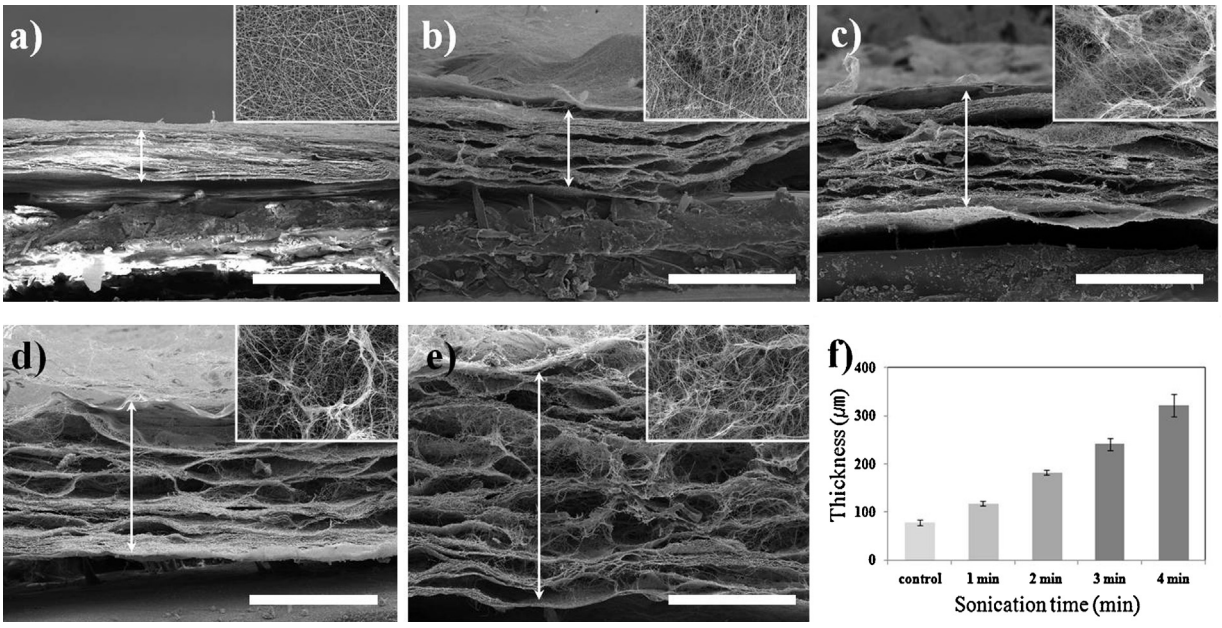

Fig. 3. Cross sectional FE-SEM image of chitosan nanofibers mat after ultra-sonication treatment according to time: (a) non-sonicated (scale bar: 100 μm), (b)–(e) 1 min, 2 min, 3 min and 4 min sonicated using ultra-sonicator (scale bar: 200 μm), and (f) distribution of chitosan nanofibers mat thickness. Inset images are surface morphology of chitosan nanofibers mat. The arrow marks the thickness of the chitosan nanofibers mat.

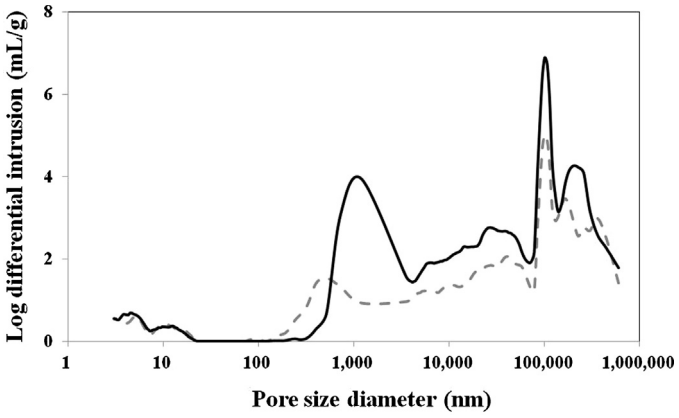

Fig. 4. Porosity and pore size distribution of non-sonicated (dash line) and 1 min sonicated (solid line) chitosan nanofibers mat using mercury porosimetry.

Therefore, the chitosan mats required neutralization to prevent their dissolution in aqueous medium. 3 M NaOH and 5 M Na_2CO_3 solutions are often used for the neutralization of chitosan materials; however, these agents require at least 3 h of incubation in order to achieve the required results (Sangsanoh & Supaphol, 2006). Here, three different alkaline solutions were assessed in order to reduce the treatment time required for sufficient for neutralization. Fig. 1(b)–(d) shows FE-SEM images of samples that were treated with 5 M Na_2CO_3, 29% aqueous NH_3, and 3 M NaOH in aqueous methanol for 3 h, 30 min, and 10 min, respectively. After neutralization, the average diameters of the chitosan nanofibers were 444.3 ± 59.5, 401.8 ± 43.9, and 356.1 ± 34.6 nm, respectively (Fig. 1(e)). Treatment with Na_2CO_3 and NH_3 resulted in collapse of the nanofiber structure, but the average diameter of the NaOH neutralized chitosan nanofibers was observed to be similar to that of the as-spun mat. However, the chitosan nanofiber structure was destroyed after neutralization using 3 M NaOH in aqueous ethanol (data not shown), in contrast to when aqueous methanol was used.

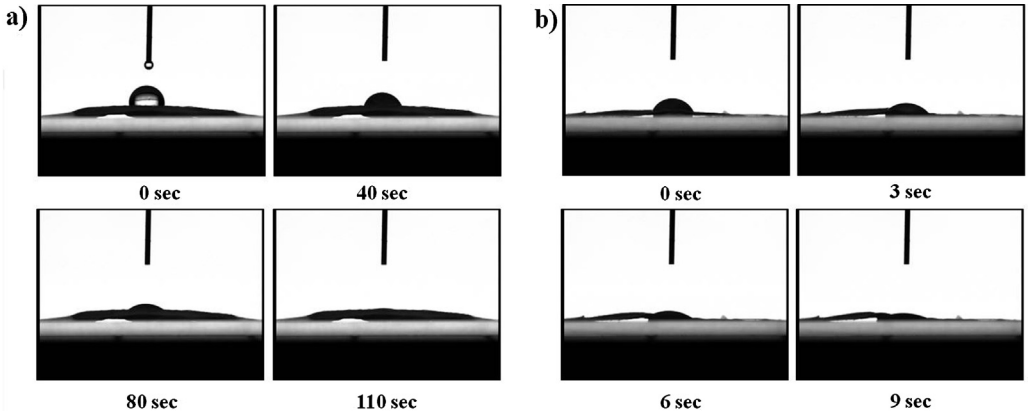

Fig. 5. Initial contact angle and adsorption time of water droplets on (a) the non-sonicated chitosan nanofibers mat; (b) the sonicated chitosan nanofibers mat with smooth surface.

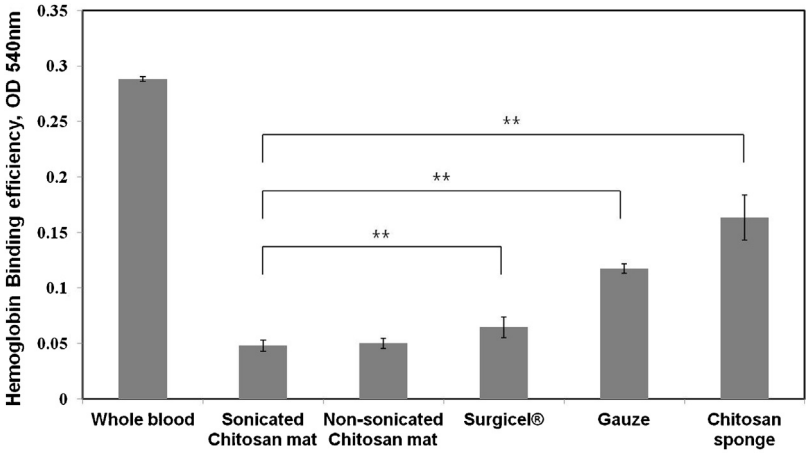

Fig. 6. The hemoglobin binding efficiency of the sonicated chitosan nanofibers, the non-sonicated chitosan nanofibers, the Surgicel®, the commercial gauze, and chitosan sponge scaffolds (**$p < 0.01$).

The neutralization process employing NaOH in methanol was relatively low-cost and faster than the use of the other alkali solutions.

The mechanical properties of tissue engineering scaffolds are extremely important, as the cells require an appropriate substrate before new tissue can be formed (Agarwal, Wendorff, & Greiner, 2008). Fig. 2 shows typical stress–strain curves of the as-spun, neutralized, and sonicated chitosan nanofiber mats in the wet and dry state. It was found that the as-spun chitosan nanofibers mat had a tensile strength of 2.41 MPa, an elastic modulus of 0.61 MPa, and an elongation at break of 14.1%. The data demonstrate that the

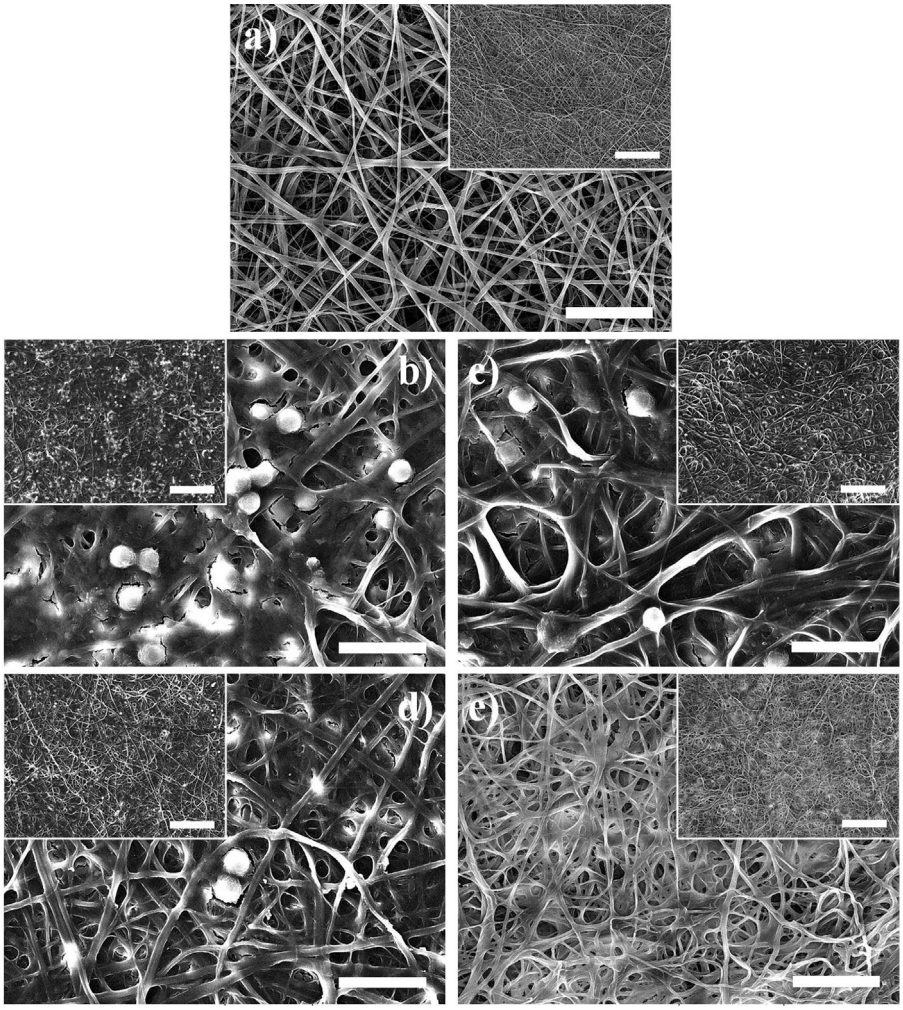

Fig. 7. FE-SEM image of platelets adhesion on the chitosan nanofibers mat. (a) Chitosan nanofibers after 10 min of absorption in PBS, (b) and (c) sonicated and non-sonicated chitosan nanofibers after 10 min of absorption, (d) and (e) sonicated and non-sonicated chitosan nanofibers after 1 min of absorption, respectively. Inset image is low-magnification (scale bar: 10 μm, inset scale bar: 50 μm).

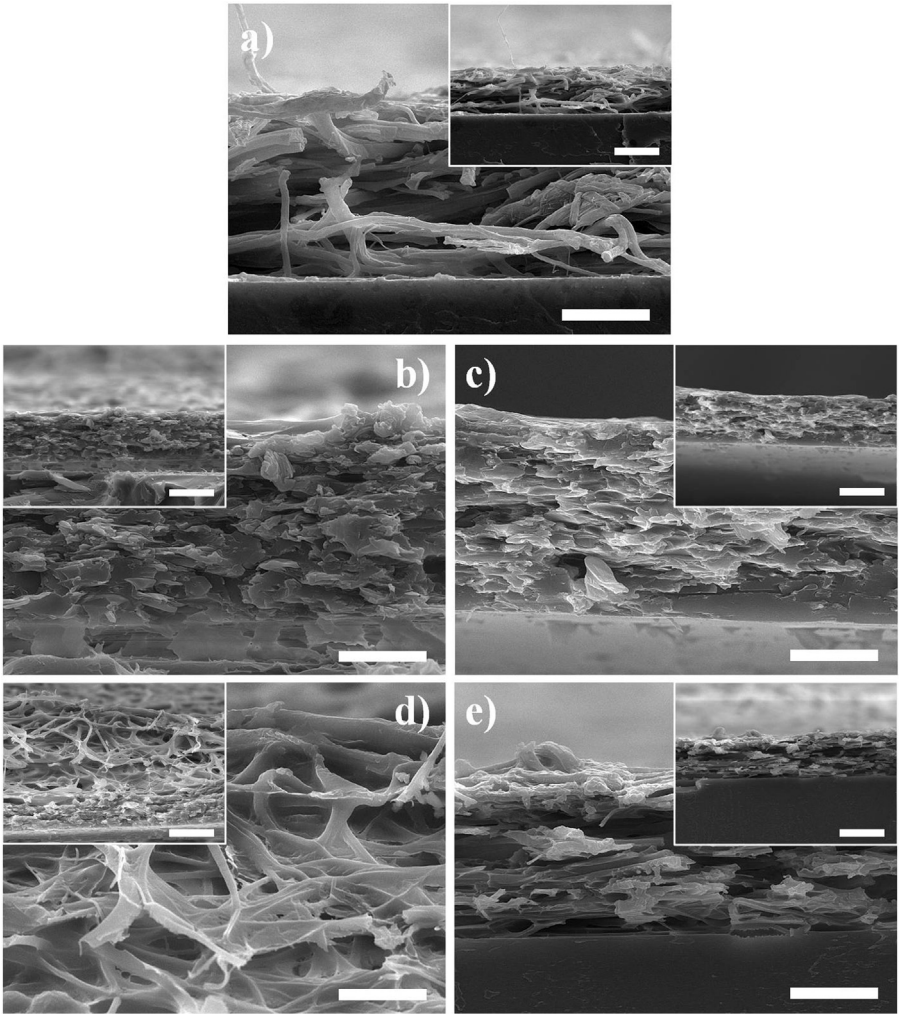

Fig. 8. Cross-sectional image of platelets adhesion on the chitosan nanofibers mat. (a) Chitosan nanofibers after 10 min of absorption in PBS, (b) and (c) sonicated and non-sonicated chitosan nanofibers after 10 min of absorption, (d) and (e) sonicated and non-sonicated chitosan nanofibers after 1 min of absorption, respectively. Inset image is low-magnification (scale bar: 5 μm, inset scale bar: 10 μm).

neutralized chitosan nanofiber mat in the dry state was very brittle, exhibiting a break strain as low as 4.1%, high stress at break (4.42 MPa), and an elastic modulus of 2.32 MPa. The neutralized mat was also tested in a wet state, with the results showing a significant difference in the stress–strain behavior relative to the dry samples. The break stress was lower (1.73 MPa) by an order of magnitude compared to the dry samples, and the elongation at break was higher (17.1%). In comparison, the mechanical properties of the material that was sonicated for 1 min showed tensile strengths of 2.56 and 0.65 MPa, elastic moduli of 1.27 and 0.03 MPa, and elongations at break of 4.1 and 15.3% for the dry and wet states, respectively.

It has previously been shown that ultra-sonication can be employed to control the pore size and thickness of a nanofiber mat in order to enhance water absorption time and cell viability. When the synthetic polymer poly(L-lactic acid) (PLLA) was used, the porous 3D scaffolds was fabricated using ultra-sonication with 150 W energy (Lee et al., 2011); however, this was not effective for producing a porous nanofiber structure from the natural chitosan polymer used in the present study. This is likely because of the strong intermolecular hydrogen bonding between the chitosan molecules of nanofibers. Thus, a higher energy of 225 W was used to obtain a porous chitosan nanofiber mat. Fig. 3 shows the differences in surface and cross section morphology of the nanofiber mats according to ultra-sonication time. The thickness of the non-sonicated mat was found to be 78.4 ± 6.3 μm (Fig. 3(a)), with a dense, bead-free mesh structure with random nanofibers (inset image). As shown in Fig. 3(b)–(e), the thicknesses of the chitosan mats were dramatically increased with sonication time, with values of 117.9 ± 5.2, 181.9 ± 4.7, 240.8 ± 12.8, and 321.3 ± 23.2 μm for 1, 2, 3, and 4 min sonication, respectively. The maximum thickness achieved using the sonication was 300% greater than for the non-sonicated mat. In addition, the pore size of the mat surface was increased after ultra-sonication treatment (inset images), although there was little difference observed between the 1 min and 4 min samples.

As shown in Fig. 4, mercury porosimetry was used to quantitatively compare the pore size distribution and porosity of the non-sonicated and sonicated chitosan nanofiber mats. The pore size for the non-sonicated mat was approximately 470 nm, while that of the sonicated mat was much higher at around 1.1 μm. Moreover, the porosity of the non-sonicated mat was 79.9%, indicating a dense mesh structure. The total pore volume was 6.2 ml/g, and the total pore area was 212.6 m^2/g. After ultra-sonication for 1 min, the total pore area increased, and the porosity and pore volume increased to 97.2% and 9.1 ml/g, respectively, indicating that the chitosan nanofiber mat expanded due to the sonication, forming large pores.

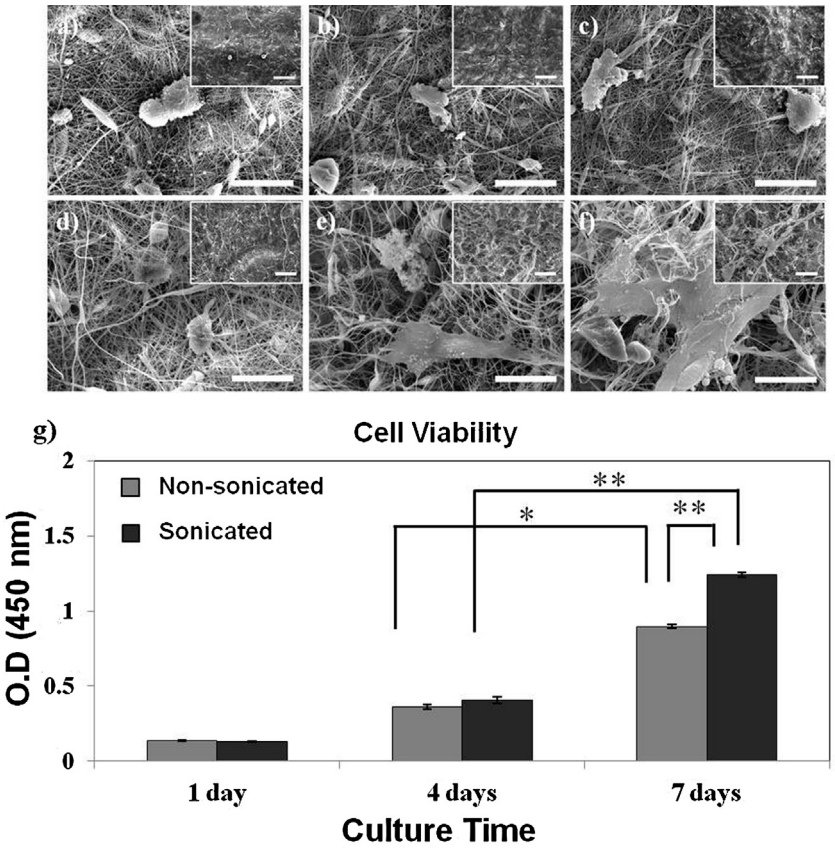

Fig. 9. FE-SEM images of normal human dermal fibroblast cells (NHDFs) cultured on (a)–(c) non-sonicated and (d)–(f) sonicated chitosan nanofibers mat after 1, 4 and 7 days of culture. (g) The viability of NHDFs on chitosan nanofibers mat during 7 days. Inset image is low-magnification (scale bar: 20 μm, inset scale bar: 50 μm; $^{*}p < 0.05$, $^{**}p < 0.01$).

Hemostatic materials should be capable of providing rapid and effective control of bleeding; hence their initial blood absorption times should be low (Neuffer et al., 2004). Fig. 5 shows the water absorption time and initial contact angle on the non-sonicated and sonicated chitosan nanofiber mats. The results indicate that the non-sonicated mat was less hydrophilic, with a water contact angle of 82° and a complete water absorption time of 110 s. The sonicated mat exhibited a lower water contact angle of 54° and a greatly superior water absorption time of 9 s. The initial high water contact angle of the nanofiber mat was due to the dense nanofiber structure (Tang et al., 2009; Zhu, Cui, Li, & Jin, 2008), but on sonication, the angle decreased, indicating the formation of a less dense material with a larger pore size and greater porosity.

After achieving such promising results using water, the next step was to assess how the nanofiber mats interacted with blood. Thus, the blood clotting efficiency of the sonicated material was evaluated using methodology previously reported in the literature (Madhumathi et al., 2010; Shih et al., 2006). Fig. 6 shows the results of the blood clotting (hemoglobin binding) experiments, where a lower hemoglobin binding efficiency indicates higher thrombogenic activity of the sample (Sun et al., 2009). The samples were incubated with rabbit whole blood containing an anticoagulant for 10 min at 37 °C, and then the binding efficiency was quantified by measuring the absorption (OD) at 540 nm. The hemoglobin binding for the sonicated nanofiber mat was found to be lower than for the Surgicel®, the commercial gauze, and the chitosan sponge used as an additional control. The hemoglobin binding for the sonicated and non-sonicated chitosan nanofiber mats were similar; however, because the initial absorption time of blood is highly important for achieving hemostasis, the level of platelet adhesion and clot formation were assessed after a shorter blood contact time. Figs. 7 and 8 show FE-SEM images demonstrating the adhesion of platelets and clot formation on sonicated and non-sonicated chitosan nanofiber mats after different blood absorption times. As a control group, PBS was used instead of whole blood (Fig. 7(a)). In Fig. 7(b) and (c), fewer platelets can be seen to have adhered to the non-sonicated chitosan nanofiber mat in comparison with the sonicated material. In addition, the number of platelets observed on sonicated and non-sonicated chitosan mats after 10 min blood absorption time was higher than after 1 min. Fig. 8 shows a cross-sectional image of the same samples as shown in Fig. 7. It can be seen that the blood clot was greatly increased by infiltrated blood at the inner part of the chitosan mat produced by 10 min sonication (Fig. 8(b)). After 1 min blood adsorption time, the difference in the level of platelet adhesion and deposited clot formation between the sonicated and non-sonicated chitosan nanofiber mats can be easily discerned from the cross-sectional SEM images. The clot formation after 1 min of blood contact was greater for the sonicated material (Fig. 8(d)) than for the non-sonicated (Fig. 8(e)). The appearance of the non-sonicated chitosan mat (1 min) was similar to that of the mat that was immersed in PBS (Fig. 8(a)), indicating vary little blood clot formation on this material. The increase in platelet adhesion on the sonicated material was likely due to rapid attachment of blood proteins such as immunoglobulin to the chitosan nanofiber mat with improved pore size and porosity. The results from the blood contacting studies are in agreement with those shown in Fig. 5 for water absorption. In both cases, the sonicated mat, with its higher pore size and porosity, had a much shorter liquid absorption time. These results indicate that the sonicated chitosan nanofiber mat has great potential to be used as a hemostatic agent.

To investigate the effects of pore size on cell viability for potential tissue engineering applications, NHDFs were cultured

on sonicated and non-sonicated chitosan nanofiber mats for 1, 4, and 7 days. Fig. 9 shows that the optical density (OD) values that represent the number of cells present on the non-sonicated and sonicated chitosan mats demonstrated that there was a similar cell growth pattern after 1 day of culture. However, after 7 days, the OD value from the sonicated sample (1.24 ± 0.02) was higher than for the non-sonicated sample (0.89 ± 0.02). This demonstrates that the cells cultured on the sonicated chitosan nanofiber mat had an approximately 1.4-fold higher viability than those on the non-sonicated mat under the same culture conditions. This result was likely due to the enhanced cellular attachment and mass transport of nutrients and metabolic waste possible for the sonicated mat, leading to higher cell proliferation.

Therefore, the sonicated chitosan nanofiber mat, with its enhanced porosity and wettability, would be a good candidate for use as both a tissue engineering scaffold and a hemostatic material, providing higher cell adhesion and growth in addition to rapid blood coagulation.

4. Conclusions

Pure chitosan nanofibers were prepared by electrospinning, with control over pore size and mat thickness achieved using ultrasonication. The optimum neutralization conditions for the chitosan nanofibers were identified by testing various alkaline solutions. The thickness and porosity of the mats could be controlled by varying the ultra-sonication time. The sonicated chitosan nanofiber mats were more porous and the water absorption time was improved from 110 s to 9 s. The blood clotting efficiency of the sonicated chitosan nanofiber mat was superior to that observed for the Surgicel®, and chitosan sponge controls. Additionally, cell viability on the sonicated mat was found to be 1.4-fold higher than for the non-sonicated mat. These results suggest that the sonicated chitosan nanofiber mat has great potential for use in tissue engineering applications and as a hemostatic wound dressing.

Acknowledgments

This research was supported by Basic Science Research Program (NRF-2012R1A1A2008206) and by National Nuclear R&D Program through the National Research Foundation of Korea (NRF) funded by the Ministry of Education, Science and Technology and by Industrial Strategic Technology Development Program (10035291, Multi-Functional Medical Fiber Complex Technology) funded by the Ministry of Knowledge Economy (MKE, Korea)

References

Agarwal, S., Wendorff, J. H., & Greiner, A. (2008). Use of electrospinning technique for biomedical applications. *Polymer*, *49*, 5603–5621.

Baldrick, P. (2010). The safety of chitosan as a pharmaceutical excipient. *Regulatory Toxicology and Pharmacology*, *56*, 290–299.

Bhattarai, N., Li, Z., Gunn, J., Leung, M., Cooper, A., Edmondson, D., et al. (2009). Natural–synthetic polyblend nanofibers for biomedical applications. *Advanced Materials*, *21*, 2792–2797.

Chen, Z. G., Wang, P. W., Wei, B., Mo, X. M., & Cui, F. Z. (2010). Electrospun collagen-chitosan nanofibers: A biomimetic extracellular matrix for endothelial cell and smooth muscle cell. *Acta Biomaterialia*, *6*, 372–382.

Cooper, A., Jana, S., Bhattarai, N., & Zhang, M. (2010). Aligned chitosan-based nanofibers for enhanced myogenesis. *Journal of Materials Chemistry*, *20*, 8904–8911.

Dash, M., Chiellini, F., Ottenbrite, R. M., & Chiellini, E. (2011). Chitosan-A versatile semi-synthetic polymer in biomedical applications. *Progress in Polymer Science*, *36*, 981–1014.

Desai, K., Kit, K., Li, J., & Zivanovic, S. (2008). Morphological and surface properties of electrospun chitosan nanofibers. *Biomacromolecules*, *9*, 1000–1006.

Doshi, J., & Reneker, D. H. (1995). Electrospinning process and applications of electrospun fibers. *Journal of Electrostatics*, *35*, 151–160.

Dzenis, Y. (2004). Spinning continuous nanofibers for nanotechnology. *Science*, *304*, 1917–1919.

Elsabee, M. Z., Naguib, H. F., & Morsi, R. E. (2012). Chitosan based nanofibers, review. *Materials Science and Engineering C*, *32*, 1711–1726.

Fischer, T. H., Thatte, H. S., Nichols, T. C., Bender-Neal, D. E., Bellinger, D. A., & Vournakis, J. N. (2005). Synergistic platelet integrin signaling and factor XII activation in poly-N-acetyl glucosamine fiber-mediated hemostasis. *Biomaterials*, *26*, 5433–5443.

Geng, X., Kwon, O. H., & Jang, J. (2005). Electrospinning of chitosan dissolved in concentrated acetic acid solution. *Biomaterials*, *26*, 5427–5432.

Greiner, A., & Wendorff, J. H. (2007). Electrospinning: A fascinating method for the preparation of ultrathin fibers. *Angewandte Chemie International Edition*, *46*, 5670–5703.

Gu, R., Sun, W., Zhou, H., Wu, Z., Meng, Z., Zhu, X., et al. (2010). The performance of a fly-larva shell derived chitosan sponge as an absorbable surgical hemostatic agent. *Biomaterials*, *31*, 1270–1277.

Hubbel, J. A. (1995). Biomaterials in tissue engineering. *Nature Biotechnology*, *13*, 565–576.

Janvikul, W., Uppanan, P., Thavornyutikarn, B., Krewraing, J., & Prateepasen, R. (2006). In vitro comparative hemostatic studies of chitin, chitosan, and their derivatives. *Journal of Applied Polymer Science*, *102*, 445–451.

Jayakumar, R., Prabaharan, M., Nair, S. V., & Tamura, H. (2010). Novel chitin and chitosan nanofibers in biomedical applications. *Biotechnology Advances*, *28*, 142–150.

Jayakumar, R., Chennazhi, K. P., Muzzarelli, R. A. A., Tamura, H., Nair, S. V., & Selvamurugan, N. (2010). Chitosan conjugated DNA nanoparticles in gene therapy. *Carbohydrate Polymers*, *79*, 1–8.

Kang, P. L., Chang, S. J., Manousakas, I., Lee, C. W., Yao, C. H., Lin, F. H., et al. (2011). Development and assessment of hemostasis chitosan dressings. *Carbohydrate Polymers*, *85*, 565–570.

Kean, T., & Thanou, M. (2010). Biodegradation, biodistribution and toxicity of chitosan. *Advanced Drug Delivery Review*, *62*, 3–11.

Kim, M. S., Park, S. J., Gu, B. K., & Kim, C. H. (2012). Inter-connecting pores of chitosan scaffold with basic fibroblast growth factor modulate biological activity on human mesenchymal stem cells. *Carbohydrate Polymers*, *87*, 2683–2689.

Kim, O. Y., Kim, S. J., Song, Y. S., Jo, E. H., Hwang, J. H., Bae, J. Y., et al. (2011). Purification and characterization of alginate for the application of regenerative medicine. *International Journal of Tissue Regeneration*, *2*, 13–20.

Klossner, R. R., Queen, H. A., Coughlin, A. J., & Krause, W. E. (2008). Correlation of chitosan's rheological properties and its ability to electrospun. *Biomacromolecules*, *9*, 2947–2953.

Lee, J. B., Jeong, S. I., Bae, M. S., Yang, D. H., Heo, D. N., Kim, C. H., et al. (2011). Highly porous electrospun nanofibers enhanced by ultrasonication for improved cellular infiltration. *Tissue Engineering: Part A*, *17*, 2695–2702.

Lee, O. J., Lee, J. M., Jin, H. J., & Park, C. H. (2010). The pilot study for the development of the artificial dermis using silk fibroin. *International Journal of Tissue Regeneration*, *1*, 68–73.

Lord, M. S., Cheng, B., McCarthy, S. J., Jung, M. S., & Whitelock, J. M. (2011). The modulation of platelet adhesion and activation by chitosan through plasma and extracellular matrix proteins. *Biomaterials*, *32*, 6655–6662.

Madhumathi, K., Sudheesh Kumar, P. T., Abhilash, S., Sreeja, V., Tamura, H., Manzoor, K., et al. (2010). Development of novel chitin/nanosilver composite scaffolds for wound dressing applications. *Journal of Materials Science: Materials in Medicine*, *21*, 807.

Malette, W. G., Quigley, H. J., Gaines, R. D., Johnson, N. D., & Rainer, G. (1983). Chitosan: A new hemostatic. *Annals Thoracic Surgery*, *36*, 55–58.

Muzzarelli, R. A. A. (2009). Chitins and chitosans for the repair of wounded skin, nerve, cartilage and bone. *Carbohydrate Polymers*, *76*, 167–182.

Muzzarelli, R. A. A. (2011). Chitosan composites with inorganics, morphogenetic proteins and stem cells, for bone regeneration. *Carbohydrate Polymers*, *83*, 1443–1445.

Muzzarelli, R. A. A., Greco, F., Busilacchi, A., Sollazzo, V., & Gigante, A. (2012). Chitosan, hyaluronan and chondroitin sulfate in tissue engineering for cartilage regeneration: A review. *Carbohydrate Polymers*, *89*, 723–739.

Neuffer, M. C., McDivitt, J., Rose, D., King, K., Cloonan, C. C., & Vayer, J. S. (2004). Hemostatic dressings for the first responder: A review. *Military Medicine*, *169*, 716–720.

Ohkawa, K., Cha, D., Kim, H., Nishida, A., & Yamamoto, H. (2004). Electrospinning of chitosan. *Macromolecular Rapid Communications*, *25*, 1600–1605.

Ong, S. Y., Wu, J., Moochhala, S. M., Tan, M. H., & Lu, J. (2008). Development of a chitosan-based wound dressing with improved hemostatic and antimicrobial properties. *Biomaterials*, *29*, 4323–4332.

Park, H. N., Lee, J. B., & Kwon, I. K. (2010). Electrospun nanofibers using biomacromolecules and their applications as tissue engineered scaffolds. *International Journal of Tissue Regeneration*, *1*, 10–20.

Reneker, D. H., & Chen, I. (1996). Nanometre diameter fibres of polymer, produced by electrospinning. *Nanotechnology*, *7*, 216.

Sangsanoh, P., & Supaphol, P. (2006). Stability improvement of electrospun chitosan nanofibrous membranes in neutral or weak basic aqueous solutions. *Biomacromolecules*, *7*, 2710–2714.

Sangsanoh, P., Suwantong, O., Neamnark, A., Cheepsunthorn, P., Pavasant, P., & Supaphol, P. (2010). In vitro biocompatibility of electrospun and solvent-cast chitosan substrata towards schwann, osteoblast, keratinocyte and fibroblast cells. *European Polymer Journal*, *46*, 428–440.

Schiffman, J. D., & Schauer, C. L. (2008). A review: Electrospinning of biopolymer nanofibers and their applications. *Polymer Reviews*, *48*, 317–352.

Shih, M. F., Shau, M. D., Chang, M. Y., Chiou, S. K., Chang, J. K., & Cherng, J. Y. (2006). Platelet adsorption and hemolytic properties of liquid crystal/composite polymers. *International Journal of Pharmaceutics*, *327*, 117–125.

Sun, Z. J., Wu, L., Huang, W., Zhang, X. L., Lu, X. L., Zheng, Y. F., et al. (2009). The influence of lactic on the properties of poly(glycerol-sebacate-lactic acid). *Materials Science and Engineering: C*, *29*, 178–182.

Tang, H., Wang, H., & He, J. (2009). Superhydrophobic titania membranes of different adhesive forces fabricated by electrospinning. *Journal of Physical Chemistry C*, *113*, 14220–14224.

Ueno, H., Mori, T., & Fujinaga, T. (2001). Topical formulations and wound healing applications of chitosan. *Advanced Drug Delivery Reviews*, *52*, 105–115.

Xie, J., MacEwan, M. R., Li, X., Sakiyama-Elbert, S. E., & Xia, Y. (2009). Neurite outgrowth on nanofiber scaffolds with different orders, structures, and surface properties. *ACS Nano*, *3*, 1151–1159.

Yang, J., Tian, F., Wang, Z., Wang, Q., Zeng, Y. J., & Chen, S. Q. (2008). Effect of chitosan molecular weight and deacetylation degree on hemostasis. *Journal of Biomedical Materials Research Part B: Applied Biomaterials*, *84B*, 131–137.

Zhu, X., Cui, W., Li, X., & Jin, Y. (2008). Electrospun fibrous mats with high porosity as potential scaffolds for skin tissue engineering. *Biomacromolecules*, *9*, 1795–1801.